wjert, 2023, Vol. 9, Issue 7, 38-42. Original Article ISSN 2454-695X

World Journal of Engineering Research and Technology

WJERT

www.wjert.org SJIF Impact Factor: 5.924

FORMATION AND STUDY OF THE PROPERTIES OF THE COMPOUND OF IRON DISILICIDE IN SINGLE-CRYSTAL SILICON

Kh. S. Daliev*[1] and Z. M. Khusanov[2]

[1]Branch of the Federal State Budgetary Educational Institution of Higher Education "National Research University MPEI.

[2]Institute of Semiconductor Physics and Microelectronics at NUUz (Tashkent), Uzbekistan.

Article Received on 31/04/2023 Article Revised on 21/05/2023 Article Accepted on 11/06/2023

***Corresponding Author**
Kh. S. Daliev
Branch of the Federal State Budgetary Educational Institution of Higher Education "National Research University MPEI.

ABSTRACT

The results of the diffusion capacity of iron in silicon are presented. It is known that, among transition metals, the study of the properties of the interaction of iron (Fe) atoms in silicon is of great interest.

KEYWORDS: Iron disilicide, diffusion, magnetron, compounds, spectrum, complexes, temperature.

INTRODUCTION

In iron structures, iron disilicide compounds can be formed after the introduction of iron atoms by diffusion, which leads to local thinning of the oxide and an increase in the surface roughness of single-crystal silicon.[1–2] In depletion regions of MOS devices, iron acts as an efficient minority carrier generation site,[3,4] increasing the dark current of charge-coupled devices (CCDs).[9] and causing update failures in dynamic random-access memory (DRAM) chips.[6] Generation-recombination centers associated with dissolved iron and its disilicide complexes increase leakage currents in any reverse biased junction, which increases energy consumption and heat generation.[5,6] In single-crystal and polycrystalline photovoltaic devices, iron contamination leads to the creation of recombination centers, which reduce the diffusion length of minority charge carriers and, consequently, the efficiency of the solar cell.[16] As device sizes continue to shrink, device performance becomes more susceptible to defects and contamination.[7,8] Because ultrapure technology to reduce surface iron contamination to below $10^{10} \div 10^{11}$ cm^{-2} is extremely expensive, understanding the

mechanisms of iron contamination, the detrimental role of iron in silicon devices, is becoming increasingly important. and allowable limits for iron contamination for each specific process. This requirement aroused great interest in the physics of iron in silicon.

The main obstacle in establishing a consistent experimental picture of 3d - transition metals in silicon and, in particular, iron, arises from the high diffusivity of these elements. Iron remains mobile at room temperature and can diffuse rapidly at temperatures above 100 ^{0}C. Since interstitial iron is positively charged in p-Si at room and slightly elevated temperatures, it readily pairs with negatively charged defects such as shallow acceptors. The high reactivity of iron was confirmed by electron paramagnetic resonance (EPR) studies, in which more than 30 iron complexes were detected, and electrical measurements, which revealed about 20 deep levels associated with iron.

EXPERIMENT

The study of the electrical and photoelectric properties of silicon alloyed with iron elements is increasingly attracting the attention of scientists and specialists with its new, previously unknown electrical and photoelectric properties.

Iron films are deposited on the surface of single-crystal silicon by magnetron ion sputtering from pure Fe targets in an Ar atmosphere.[10] Subsequent thermal annealing was carried out in ampoules at 300°C to 1200°C for 10 hours. In these films, we observed the formation of iron disilicide $FeSi_2$ using the Raman spectrum and scanning electron microscope - AFM. To study the surface morphology of the obtained materials, an EVO MA 10 scanning electron microscope (SEM) was used (Fig. 1). A high-resolution analytical scanning electron microscope is designed for a wide range of research tasks and quality control at the submicron level [11; c. 287-289].

RESULTS AND DISCUSSION

Using a scanning electron microscope after deposition of iron and after diffusion in silicon. Structure studies carried out on a transmission electron microscope are shown in Fig.1. The comparison made made it possible to conclude that microcrystalline inclusions are precipitates of various phases of $FeSi_2$. The maximum size of precipitates is 20÷25 nm and changes insignificantly with increasing iron concentration.

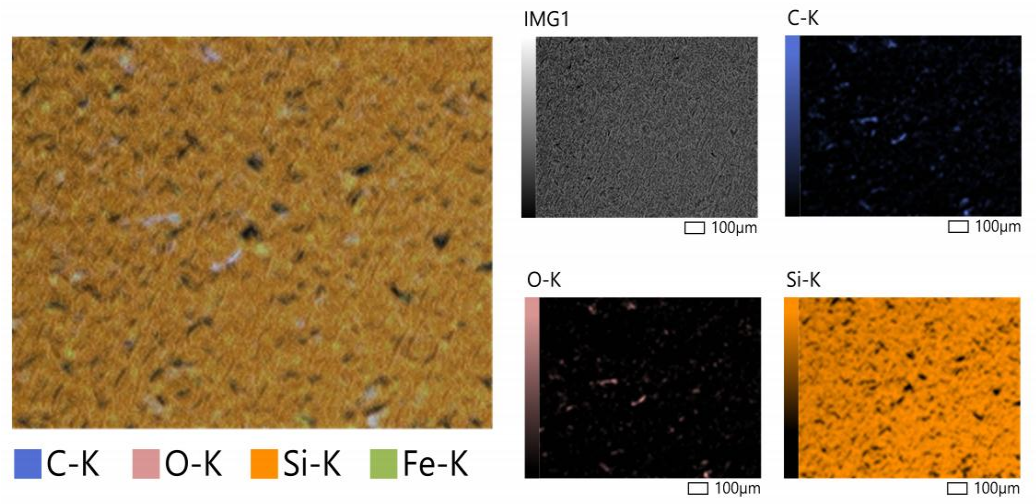

Fig. 1: Electron microscopic image of the film, taken in the bright field mode, Fe = 2.4 • 10^{21} cm^{-3}.

However, an approximately twofold increase in the iron content from $1.1 \cdot 10^{21}$ to $2.4 \cdot 10^{21}$ cm^3 leads to an increase in the density of $FeSi_2$ precipitates from $7 \cdot 10^{10}$ to $2.5 \cdot 10^{11}$ cm^{-2}.

The structure of the samples was studied by Raman spectroscopy (Fig. 2). Raman spectra were obtained using an automatic setup based on a DFS-24 spectrometer. All spectra were recorded at 300 K in the range 0÷600 cm^{-1} with a resolution of 3 cm^{-1}. An argon laser (λ = 514.5 nm) was used as an excitation source.

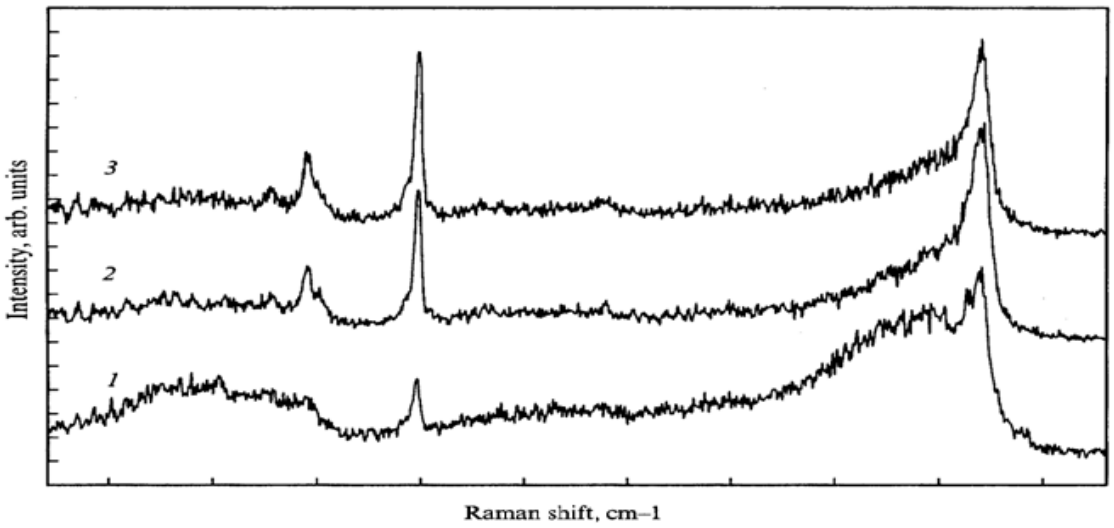

Fig. 2: Raman spectra of films with different iron concentrations N_{Fe}, cm^{-3}: 1-1.4 · 10^{21}, 2-2.6 · 10^{21}, 3-2.8 · 10^{21}.

The Raman spectra of samples after thermal annealing are shown in Figs. 2. We observed 4 strong lines in the spectra, which are located at 195, 247 and 480÷520 cm^{-1}. The 480÷520 cm^{1} lines belong to the amorphous and microcrystalline silicon phase and correspond to the TO-phonon mode. From fig. Figure 2 shows that the spectrum in the region 400÷600 cm^{-1} consists of two lines with significantly different widths. The broad line centered at about 480 cm^{-1} belongs to the amorphous phase (amorphous binder fabric, network and (or) amorphous surface between microcrystalline grains). A narrow line centered at ~520 cm^{-1} indicates the presence of a microcrystalline phase of silicon with iron compounds.

As for the lines located at 196 and 247 cm^{-1}, they are due to the presence of s-$FeSi_2$. c - The iron disilicide phase crystallizes into the orthorhombic space group DC. For Raman spectroscopy, factorial group analysis predicts 12 active internal modes, which are likely to produce most of the 14 Raman lines.[12] In addition, the Raman susceptibility of the three Ag modes should not change when the polarization of the exciting field rotates relative to the polarization of the scattered light. This takes place in the case of the three most intense lines of the transversely polarized spectrum at 197.253 and 346 cm^{-1}, which were observed in a $FeSi_2$ film with a thickness of 1 μm located on a FeSi substrate. Lines at 178, 201 and 252 cm^{-1} were measured for bulk polycrystalline $FeSi_2$. In the case of a $FeSi_2$ film with a thickness of 200 nm, which was grown on a Si substrate, the authors of.[12,13] observed the main lines at 176, 195/200, and 247 cm^{-1}.

It should be noted that in all cases the peak located at 247 cm^{-1} (Ag mode) was the most intense, and for this reason, many authors focus their attention only on this peak. As can be seen from fig. 2, the intensity of the peak at 247 cm^{-1} increases with increasing Fe concentration, which can be explained by an increase in the amount of the synthesized phase in -$FeSi_2$. It should also be noted that an increase in the Fe concentration leads to a decrease in the intensity of the broad line at about 480 cm^{-1}, which is attributed to the TO phonon mode of amorphous silicon.

CONCLUSIONS

In the present work, the formation of $FeSi_2$ iron disilicide in single-crystal silicon films doped with iron was observed. Iron-doped silicon films were obtained by magnetron sputtering from iron targets in an argon atmosphere. Subsequent thermal annealing at T = 800°C for 10 hours led to the formation of iron disilicide $FeSi_2$ with different formation phase and compounds. The solubility of iron in its own silicon is well known. However, data on the solubility of iron

in moderately and heavily doped n-type silicon are limited to a few doping levels and temperatures and require further research.

LITERATURE

1. D. Leong, M. Harry, K.J. Reeson, K.P. Homewood. Nature, 1997; 387: 686.
2. Wong-Leung, DJ Eaglesham, J. Sapjeta, DC Jacobson, JM Poate, JS Williams: J. Appl. Physical, 1998; 83: 580.
3. K. Honda, A. Osawa, T. Nakanishi: J. Electrochem. Social, 1995; 142: 3486.
4. Tardif, J.P. Jolie, T. Lardine, A. Tonti, P. Patruno, D. Levy, W. Sievert: Crystal Defects and Contamination: Their Influence and Control in Device Manufacturing, ed. B. O. Kolbezen, C. Clais, P. Stollhofer, F. Tardif (Electrochemical Society, Grenoble, France, 1993; 114.
5. G. Obermeier, D. Huber: J. Appl. Physical, 1997; 81: 7345.
6. L. Yastrzebski: IEEE Trans. Electron Dev. ED, 1982; 29: 475.
7. PJ Ward: J. Electrochem. Social, 1982; 129: 2573.
8. H.J. Schulze, BO Kolbesen: Materials and devices for power semiconductors, ed. S. J. Pirton, R. J. Schul, E. Wolfgang, F. Wren, S. Tenkoni (Materials Research Society, Warrendale, PA, 1998; 381.
9. K. Graff: Metal Impurities in Silicon Device Manufacturing (Springer, Berlin, 1995) HH Woodbury, GW Ludwig: Phys, 1960; 117: 102.
10. Muzafarova S.A. Study of photosensitive SDP structures based on cadmium telluride. // Candidate's thesis Tashkent**,** 1983.
11. G.M. Zeer, O.Yu.Fomenko, O.N. Ledyaeva. The use of scanning electron microscopy in solving actual problems // Siberian Federal University, 2009; 4(2): 287 – 293.
12. K. Lefki, P. Muret, E. Bustarret, N. Boutarek, R. Madar, J. Chewier, J. Derrien, M. Brunel. Sol. St. Commun, 1991; 80: 791.
13. A.G. Birdwell, R. Glosser, D.N. Leong, K.P. Homewood. J. Appl. Phys., 2001; 89: 965.